Cell Fate and Organogenesis in Asxl3 Mouse Model

By Shachi Salvi

Mentor

Stephanie Bielas, Ph.D., Associate Professor, Department of Human Genetics

Graduate Student Mentor

Brian McGrath, Cellular and Molecular Biology Ph.D. Candidate

Readers

Stephanie Bielas, Ph.D., Associate Professor, Department of Human Genetics

Samuel Kwon, Ph.D., Assistant Professor, Department of Molecular, Cellular, and Developmental Biology (MCDB)

Monica Dus, Ph.D., Assistant Professor, Department of MCDB

Submitted on November 30, 2020

A thesis submitted in partial fulfillment of the Degree of Bachelor of Science in Cellular and Molecular Biology with Honors

Abstract

Fate specification of multipotent cells is a highly regulated process during development of an organism to ensure that the right cell types are forming in the right locations. Many Polycomb-group genes are known to function in chromatin regulation and regulation of gene expression during early development. The *Additional Sex Combs - Like 3* (*ASXL3*) gene is a putative Polycomb-group gene thought to function in a complex called polycomb-repressive deubiqitination complex (PR-DUB), which removes a ubiquitin mark on histone H2A. The PR-DUB complex works antagonistically to polycomb repressive complex 1 (PRC1), which adds a repressive ubiquitin mark to histone H2A. These two complexes dynamically regulate the ubiquitination of H2A, and are thus termed the H2A monoubiquitination regulatory axis. Pathogenic variants in *ASXL3* have previously been identified as the genetic basis of Bainbridge Ropers Syndrome (BRS), a developmental disorder with syndromic features of autism spectrum disorder. Early work in my lab demonstrated that changes in H2A ubiquitination levels were the key molecular pathology leading to the symptoms in BRS patients. This thesis aims to further characterize the role of *ASXL3* in early development, specifically on the development of the brain and the heart. Our work with an *Asxl3* knockout mouse model has shown that *ASXL3* plays an important role in differentiation of neural progenitor cells into layer 5 upper motor neurons and in controlling proliferation and differentiation dynamics during the process of cardiogenesis. Together, our data suggests an important role for ASXL3-dependent H2AUb1 regulation during fate specification events of several organ systems.

Table of Contents

Scientific Acknowledgments

I would like to thank Dr. Stephanie Bielas for her support and guidance throughout the past three years. Her hard work and dedication to her research make her a great role model, and I would not have been able to complete this thesis without her help. I am immensely grateful for her encouragement throughout this process, and I know that I would not have been able to reach this point without her.

I would also like to thank Brian McGrath for his support and for teaching me how to carry out even the most basic protocols. I joined this lab with little research background, and Brian played an instrumental role in helping me develop my research skills. The things I have learned from him will stay with me throughout my career, and I am thankful for the time and energy he provided me with. This thesis would not exist today without his mentorship right from the beginning.

Lastly, I would like to thank the other members in my lab. Everyone has aided me in my project in one way or another, whether it be helping me troubleshoot why certain protocols went awry, providing me with tips on how to improve protocols in the future, or creating an environment that helped me learn and grow. I greatly appreciate all of their support and encouragement.

Personal Acknowledgments

I would like to thank my parents, my sister, and all my friends for everything they have done to help me reach this point. I know that without their constant and unwavering support, this thesis would not exist today. Despite not knowing the specifics about this research field, they have always listened to me talk about my project, even when they would much rather be doing something else. Knowing that these people are there to support me has encouraged me to take on greater risks and greater challenges, and they have always pushed me to the best scientist I can possibly be.

Introduction

During early development, cells are pluripotent, meaning that they have the ability to become a variety of different specialized cell types. Over time, as the organism develops, it requires certain cell types at specific times and locations. Even within organs, there is a particular structure and organization that must be achieved. In order to meet this need, pluripotent cells throughout the organism commit to particular fates via a highly orchestrated process. This process of commitment is permanent; once a cell takes on a particular fate, it cannot go back and regain its pluripotency. The irreversible nature of this differentiation process means that it is critical that cells differentiate properly and accurately. If a cell takes on the wrong fate or differentiates at the wrong time, it could have immense downstream effects on the overall development of the organism. Cell plasticity is thus very important for early development because it allows for multiple different cell types to grow from a common pool of pluripotent cells (Yadav et al. 2018). Tight regulation of the fate specification and differentiation processes is necessary to ensure that highly specialized cells are born in the right locations and at the right times.

Each specialized cell type requires a specific set of genes to be active while repressing transcriptional programs of alternative fates. One of the most common mechanisms of differentiation involves the controlled upregulation or downregulation of specific genes at the genomic level. DNA in cells is wrapped around proteins called histones to create a more compact form called chromatin that takes up less space in the nucleus. There are 5 such histones, called H1, H2A, H2B, H3, and H4. Two of each histone H2A, H2B, H3, and H4 come together to form an octamer around which DNA is wrapped. This unit is called a nucleosome. Multiple nucleosomes are linked together by histone H1, which is also called the linker histone. Modifications on these

histone proteins can result in loosening or tightening of the DNA at that site. That DNA is then more or less accessible to transcription machinery, leading to increased or decreased expression of genes at that locus. Such modifications are not permanent. Rather, they can be added and removed by various proteins and protein complexes.

Polycomb Regulation

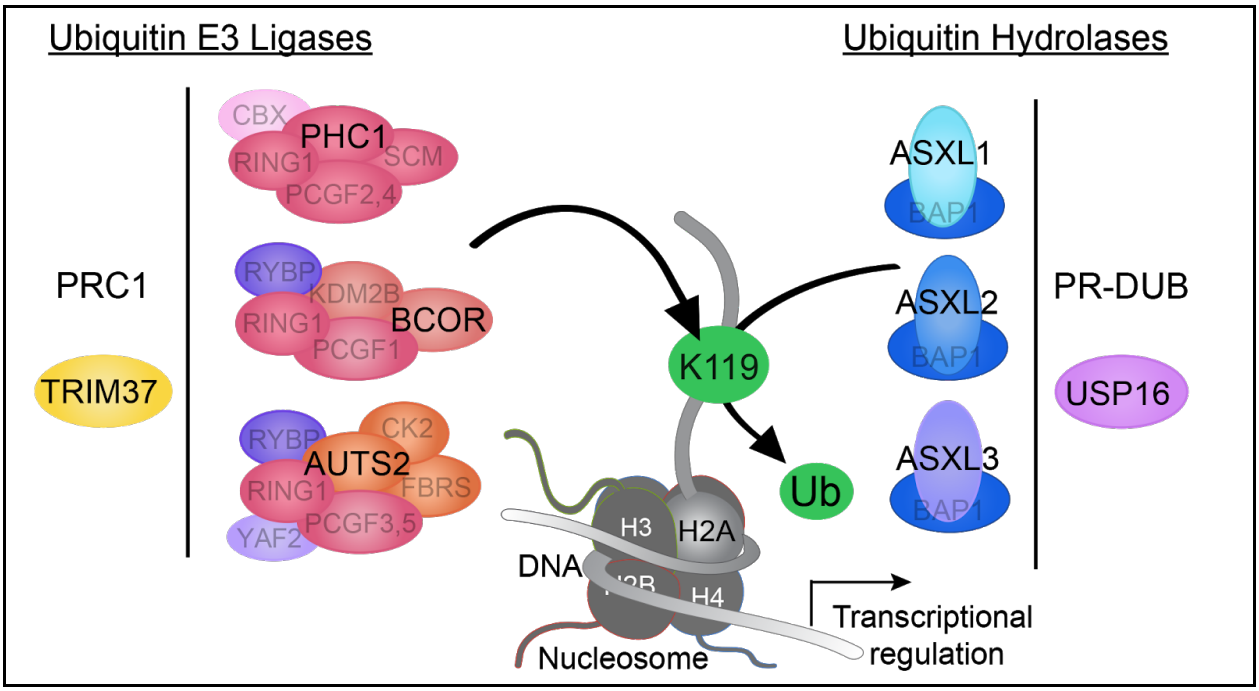

Figure 1: H2A Monoubiquitination Regulatory Axis
Diagram showing components of the H2A Monoubiquitination Regulatory Axis which dynamically regulate placement of a ubiquitin mark on histone H2A.

One important group of proteins involved in development and fate specification is Polycomb-group (PcG) proteins. PcG proteins are very conserved across organisms and are involved in the silencing of genes (Aranda et al. 2015, Schuettengruber et al. 2017). These proteins often function in very large complexes with multiple other proteins (Chittock et al. 2017). The polycomb-repressive deubiquitination complex (PR-DUB) is one such protein complex that specifically removes a ubiquitin mark from Lysine 119 on histone H2A (Fig. 1).

Monoubiquitination of histone H2A (H2AUb1) at this site is a repressive chromatin mark with transcriptional silencing effects on nearby genes. This ubiquitin mark, which is dynamically removed by PR-DUB, is initially added by polycomb-repressive complex 1 (PRC1). PRC1 is a large complex consisting of a Ring1 protein, a Polycomb Group Ring Finger protein, and multiple other important proteins. Together, PRC1 and PR-DUB form the H2A monoubiquitination regulatory axis (Fig. 1) (Srivastava et al. 2017). My lab studies this regulatory axis, with particular focus on one protein component of the PR-DUB complex, called *Additional Sex Combs - Like 3* (ASXL3).

Chromatin Regulatory Gene Asxl3

A few years ago, my lab started studying *Asxl3*, which was known to be a chromatin regulatory gene predicted to function as a component of the PR-DUB complex (Katoh et al. 2004, Scheuermann et al. 2010). Bainbridge-Ropers Syndrome (BRS), a syndromic form of Autism Spectrum Disorder (ASD), is known to be caused by *de novo* dominant mutations in *Asxl3* (Bainbridge et al. 2013, Dinwiddie et al. 2013). This gene was thought to function in a complex that removes a monoubiquitination mark from histone H2A, and early work in my lab demonstrated that changes in H2A monoubiquitination levels were a key molecular mechanism causing the symptoms associated with BRS (Srivastava et al. 2016). Individuals with BRS tend to present with global developmental delay, hypotonia, intellectual disability, and autistic features including sleep, gastrointestinal, and verbal deficits (Balasubramanian et al. 2020). It has been found that symptoms of BRS are partially penetrant, and each patient may have different clinical feature severity.

According to the Center for Disease Control and Prevention, ASD is a complex neurodevelopmental disorder affecting around 1 in 54 children in the United States. Children with ASD most often present with intellectual disabilities and social impairment, along with a myriad of other comorbidities, including Attention Deficit Hyperactivity Disorder (ADHD), anxiety disorder, and epilepsy. Previously, there was debate surrounding the causes of ASD, and it was unclear whether genetics or environmental factors played a larger role (Hultman et al. 2004). However, through the use of twin studies and whole exome sequencing analyses, it has been determined that there is a prominent genetic basis for the disorder (Bailey et al. 1995, Geschwind et al. 2007). The genes that are commonly mutated in ASD patients encode proteins that fall into three categories – chromatin regulators, transcription and splicing factors, and synaptic proteins (De Rubeis et al. 2014, Iossifov et al. 2014). It has been hypothesized that these cell and molecular activities are disrupted during early development leading to common ASD pathology (Voineagu et al. 2011). How these functional gene classes contribute to a convergent pathogenic mechanism remains unknown. *ASXl3* was identified as a high confidence ASD gene in studies that evaluated ASD cohorts in excess of 35,000 individuals (Satterstrom et al. 2020). However, virtually nothing was known about the function of ASXL3 during early development and in pathogenic mechanisms. Work in my lab focuses on characterizing the impacts of the important Polycomb group gene *Asxl3* and the H2A monoubiquitination regulatory axis on development, specifically in the brain and heart.

Corticogenesis

Previous studies investigating post-mortem tissue in animal and human ASD models indicate that ASD neuropathology results from altered growth and organization of the cerebral

cortex (Kemper et al. 1998, Bailey et al. 1998). During normal development of the cortex, a process termed corticogenesis, cortical neurons are sequentially produced by a common pool of multipotent neural progenitor cells (NPCs). Corticogenesis occurs in an inside out fashion with NPCs beginning with the production of layer 6 deep layer neurons, before restricting their fate to produce the subsequent neuronal layers. The mature cerebral cortex contains six layers (L1-6) of cortical neurons and glia, with Layer 1 on the outer periphery of the brain and Layer 6 towards the core of the brain. Mature cortical neurons in each layer display distinct morphologies, axonal projections, and gene expression patterns required for cognitive function and complex behaviors. These cortical neuron subtypes are sequentially generated through progressive lineage restriction of the common NPC pool (Desai et al. 2000, McConnell et al. 1995, Shen et al. 2006). Developmental remodeling of histone modifications, accompanied by reorganization of cell type or lineage specific transcriptional programs, is a pivotal early step in the signaling cascade that leads to acquisition of new cellular identities (Corley et al. 2007). The spatial and temporal regulation of chromatin changes influencing the transcription circuitry that determines NPC fate are only beginning to be understood. Insults at many stages of this developmental process can alter the production of neuronal subtypes, leading to downstream consequences on neuronal connections required for normal brain function (Adam et al. 2020).

Chromatin and Congenital Heart Defects

Congenital heart defects (CHD) are the most common birth defect, affecting ~1% of all live births (Triedman et al. 2016). Next-generation sequencing has been instrumental in identifying pathogenic *de novo* dominant variants in genes that encode components of chromatin modifying complexes as the basis of CHD (Zaidi et al. 2013, Homsy et al. 2015, Jin et al. 2017). In many

cases, the chromatin genes identified are also known ASD risk genes, and individuals harboring these de novo mutations have a neurodevelopmental disorder (Jin et al. 2017). The role of ASXL3 in mammalian heart development and causation of congenital heart defects is unknown. Human genetic studies and mouse models suggest an important role for Polycomb regulation during heart development (Delgado-Olguín et al. 2012; He et al. 2012a; Ai et al. 2017b; Chrispijn et al. 2019; Shirai et al. 2002; Mysliwiec et al. 2011, McGinley et al. 2014, Lee et al. 2012). Whole exome sequencing of individuals diagnosed with tetralogy of Fallot and ventricular septal defects identified compound heterozygous variants in *ASXL3* (Fu et. al 2020). When the *Asxl3* homologs *Asxl1* and *Asxl2* are knocked out, the null mice exhibit multiple congenital heart defects (McGinley et al. 2014). Together this data points to an important yet undescribed role for dynamic regulation of H2AUb1 by *Asxl3* during heart development.

Cardiogenesis

Improper formation of the heart leads to congenital heart defects. The construction of the heart starts at the early stages of embryogenesis with two cardiac progenitor populations termed the first and second heart field. The first heart field gives rise to the left ventricle and a portion of the left atrium, while the second heart field gives rise to the entire right heart, a portion of the right atrium and the outflow tracts. Initially, the cardiac progenitors give rise to a primitive heart tube which undergoes looping, chamber specification, septation, and trabeculation before forming the four-chambered heart (Buckingham et al. 2005). This highly organized process depends on complex tissue dynamics, cell-cell signaling, and temporal regulation of lineage specific gene expression programs (Bruneau et al. 2013, Miquerol et al. 2012, Srivastava et al. 2006, Olson et al. 2006). Cardiogenesis results in the generation of several specialized cell-types, including

cardiomyocytes, endocardial cells, epicardial cells, cardiac fibroblasts, and conductive cells (Cui et al. 2019, Delaughter et al. 2016). While this diversity is beginning to be uncovered, how this diversity is generated and how each cell type influences proliferation and differentiation programs remains to be determined.

Thesis Goals

My research work and that of others in my lab has focused on understanding the role of *ASXL3* in development, particularly in the development of the brain and the heart. Based on earlier research findings, we hypothesized that *ASXL3* regulates H2A monoubiquitination, the regulation of which is critical for regulation of transcription networks which determine fate for developing tissues. We hypothesized that disruptions of these key transcription networks would result in organ level defects underlying loss of *Asxl3*. To study these ideas, we engineered an *Asxl3* knockout mouse model with CRISPR-Cas9 DNA editing technology. These mice have shown multiple defects from birth, and the goals of this thesis were to characterize two of the most prominent phenotypes – developmental delays in the formation of the neocortex of the brain and hypoplastic ventricular cavities in the heart.

Materials and Methods

Animals

All experiments were performed in accordance with animal protocols approved by the Unit for Laboratory Animal Medicine (ULAM) at the University of Michigan. The Asxl3 null mice line was generated by cloning sgRNAs that target a region in exon 12 into a pX330 vector. The vectors were microinjected into fertilized eggs before being transferred into pseudopregnant C57BL/6 X DBA/2 F1 females. Topo cloning and Sanger sequencing were used to detect a unique frameshift *Asxl3* allele. The loss of Asxl3 expression was validated by qRT-PCR and western blot. *Asxl3*+/- mice were maintained on a C57BL/6 background. Heterozygous breeding was used for experiments with E0.5 established as the day of vaginal plug.

Western Blot Analysis

Total cerebral cortices from E13 *Asxl3*+/+ and *Asxl3fs/fs* mice were homogenized in RIPA buffer supplemented with protease inhibitor cocktail and phosphatase inhibitor cocktail 3 obtained from Sigma-Aldrich (P8340 and P0044; St Louis, MO, USA). Protein levels were normalized after BCA analysis. Cell lysates were separated using electrophoresis on 4-20% SDS-polyacrylamide gels and transferred to PVDF membrane (Millipore, Billerica, MA, USA). For western blot, after the transfer, the PVDF membrane was blocked with 4% milk and incubated with the following antibodies overnight. Primary antibodies used were: anti-ASXL3 (1:50, Bielas Lab), anti-ubiquityl-Histone H2A (1:2000, Cell Signaling Technology), anti-H3 (1:5000, Abcam). HRP-conjugated secondary antibodies sc-2005, sc-2030 from Santa Cruz Biotechnology (Dallas, TX, USA) were used for 1 h incubation at room temperature. Antibody incubation and

chemiluminescence detection were performed according to manufacturer's instruction [ThermoFisher Scientific (Waltham, MA, USA) cat no. 34095].

Immunohistochemistry and Counting

Brains were dissected and removed from mice at E13, E14, E15, or P0 and then kept in 4% PFA at 4℃ overnight. Brains were cryopreserved by submersion in 20% then 30% sucrose solutions and embedded in OCT cryosectioning media (Tissue-Tek, Torrance, CA). 13 μm cryosections were obtained. After thawing, sections were incubated with PBS for 15 min to wash away OCT. For antibodies that required antigen retrieval, cryosections were heated in 10 mM sodium citrate for 20 minutes at 95℃ followed by incubation at room temperature for 20 minutes and 3 PBS washes. Sections were then incubated with a normal donkey serum blocking buffer [5% NDS (Jackson ImmunoResearch), 0.1% Triton X-100, 5% BSA] for 1 hour. Subsequently, they were incubated with primary antibodies diluted in blocking buffer at 4℃ overnight, washed with PBS, and stained with secondary antibodies at room temperature for 1 hour. Slides were washed with PBS, incubated with DAPI for 5 minutes, and coverslipped with MOWIOL. Images were acquired with a Nikon A1 confocal microscope and processed with LAS X software. Cells were counted using ImageJ. Briefly, images were segmented using Trainable Weka Segmentation (Arganda-Carreras et al 2017). After thresholding the segmented images, overlapping objects were separated with watershed and then counted with analyzed particles. Primary antibodies and dilutions used: anti-TBR1 (1:200, Abcam), anti-BCL11B (1:500, Abcam), anti-SATB2 (1:100, Abcam), anti-L1CAM (1:300, Millipore), anti-SOX2 (1:500, Neuromics), anti-TBR2 (1:500, Abcam), anti-VIMENTIN (1:100, Cell Signaling Technologies).

EdU Birthdate Analysis

Females from time pregnant matings were injected with EdU (20 mg/kg) at embryonic day 13 or 14 (E13 or E14). 24 hours later or at P0, brains were dissected and removed from EdU injected pups and then kept in 4% PFA at 4℃ overnight. EdU labeling was detected in cryosections by using the Click-IT EdU imaging kit (Invitrogen, Carlsbad, CA) according to the manufacturer's instructions. After sections were incubated with Click-IT reaction cocktail, they were washed with normal donkey serum blocking buffer. Then, additional antibody staining was performed.

Cresyl Violet Staining

P0 and P2 Brains were dissected and kept in 4% PFA overnight. Fixed brains were dehydrated in a series of ethanol washes and embedded with a paraffin tissue processor. 6 μm microtome sections were dewaxed and rehydrated in series of xylene and ethanol washes, stained with 0.5% Cresyl Violet, dehydrated with ethanol, and cleared with xylene.

Collection of Cells for Single-Cell RNA Sequencing

The cerebral cortices from E13, E14, and P0 brains were dissected in Earl's balanced salt solution (EBSS). Isolated cortices were incubated with pappain (Worthington Biochemical Corporation), 5.5 mM L-cysteine-HCL, 1.1 mM EDTA, and 100 mg/ml DNase I in O_2:CO_2 equilibrated EBSS for 8 minutes at 37℃. Samples were titrated with flame tipped glass pipettes and centrifuged at 800 RCF for 5 minutes. Cells were resuspended with an ovomucoid protease inhibitor (Worthington Biochemical Corporation) and 50 mg/ml DNase I in O_2:CO_2 equilibrated EBSS then passed through a 70 micron cell strainer. Cells were centrifuged in a gradient of ovomucoid protease inhibitor at 200 RCF for 5 minutes. After, the pellet was resuspended in

NB/B27 media. Cells were counted and checked for viability with the Luna automatic cell counter (Logos Biosystems) before loading onto a Seq-Well platform.

Seq-Well Single-Cell RNA Sequencing

Seqwell was performed as described (Aicher et al. 2019, Gierahan et al. 2017). Briefly, functionalized Seq-Well arrays, containing 90,000 picowells, were loaded with barcoded beads (ChemeGenes, Wilmington, MA). 20,000 cells were loaded onto the arrays and incubated for 15 minutes. To remove residual BSA and excess cells, arrays were washed with PBS. Functionalized membranes were applied to the top of arrays, sealed in an agilent clamp, and incubated at 37℃ for 45 minutes. Sealed arrays were incubated in a lysis buffer (5 M guanidine thiocynate, 1 mM EDTA, 0.5% sarkosyl, 1% BME) for 20 minutes followed by a 45-minute incubation with hybridization buffer (2 M NaCl, 1X PBS, 8% PEG8000). Beads were removed from arrays by centrifuging at 2000xg for 5 minutes in wash buffer (2 M NaCl, 3 mM $MgCl_2$, 20 mM Tris-HCl pH 8.0, 8% PEG8000). To perform reverse transcription, beads were incubated with the Maxima Reverse Transcriptase (Thermo Scientific) for 30 minutes at room temperature followed by overnight incubation at 52℃. Reactions were treated with Exonuclease 1 (New England Biolabs) for 45 minutes at 37℃. Whole transcriptome amplification was performed using the 2X KAPA Hifi Hotstart Readymix (KAPA Biosystems). Beads were split to 1,500-2,000 per reaction and run under the following conditions: 4 Cycles (98℃, 20s; 65℃, 45s; 72℃, 3m), 12 Cycles (98℃, 20s; 67℃, 20s; 72℃, 3m), and final extension (72℃, 3m, 4℃, hold). Products were purified with Ampure SPRI beads at a 0.6X volumetric ratio then a 1.0X volumetric ratio. Libraries were prepared using the Nextera XT kit (Illumina) and libraries were sequenced on an Illumina NextSeq 75 cycle instrument.

Preprocessing of Seq-Well Data

Sequencing reads were processed into a digital gene expression matrix using Drop-seq software (Macosko et al. 2015). FASTQ files were converted into bam files before being tagged with cell and molecular barcodes and trimmed. After converting back to FASTQs, reads were aligned to mm10 with STAR. BAM files were then sorted, merged, and tagged with gene exons. Bead synthesis errors were corrected and digital gene expression matrices were generated. For downstream analysis, cells with fewer than 300 detectable genes, greater than 5,000 genes, or greater than 10% mitochondrial genes were removed. We then visualized the raw count of hemoglobin genes (Hbb-bh1, Hba-a2, Alas2, Hbb-y, Hbb-bs, Fam46c, Hbb-bt, Hba-a1, Hmbs, Fech, Slc25a37) using Violin plot to set a threshold for filtering blood cells. We normalized the data in each sample for each cell by dividing the total counts for that cell and multiplied by the 10,000. This was then natural-log transformed using log1p. After this normalization step, we selected genes showing a dispersion (variance/mean expression) larger than two standard deviations away from the expected dispersion as variable genes using the Seurat (v3.1.2) function "FindVariableGenes" for each sample. We believed that these genes have the biggest variation across cells, so focusing on these genes would give us the most information as described in the Seurat guideline. In this way, 2000 significant genes were identified using variance stabilizing transformation for each sample in different stages. We then used these most informative genes for sample alignment for each stage.

Histology and Morphometric Measurements of Cardiac Tissue

Newborn mice were sacrificed and whole bodies were fixed for 24 h in 4% paraformaldehyde, dehydrated, and embedded in paraffin. Paraffin blocks were serially sectioned at 5 μm thickness and stained with Hematoxylin/eosin and Masson's trichrome. All measurements of left ventricle free wall, right ventricle free wall, interventricular septum, left wall thickness, and right wall thickness were performed with histological sections from 9 wt, 4 het and 14 null hearts.

Results

Mouse Model Shows Disruptions in H2A Monoubiquitination Levels

In order to study the role of *Asxl3* in development, we engineered an *Asxl3* knockout mouse model using CRISPR-Cas9 DNA editing technology. Based on whole exome sequencing results, we targeted exon 12 of *Asxl3* to create clinically relevant variants that function as null alleles. Western blots for ASXL3 demonstrated the absence of protein, confirming the *Asxl3* frameshift (fs) variants function as loss-of-function alleles in null animals (Fig. 1A). Although we have studied the wild type, heterozygous, and null phenotypes, my work here specifically compares wild type and null mice. We observe skewed Mendelian ratios, perinatal lethality, and a 3-fold elevation of H2AUb1 levels in null mice (Fig. 1B, C and data not shown). The increase in H2AUb1 levels is consistent with results from patient-derived fibroblasts and *ASXL3* edited human ES cells (Srivasta et al. 2015). In accordance with *Asxl3* being a Polycomb group gene, we observe abnormalities in multiple organ systems. Phenotypes include a homeotic transformation, cardiac defects, and nervous systems defects. *Asxl3* null mice display drooping forelimbs and abnormal body curvature indicative of a neuromuscular defect (Fig. 1D) (Turgeon et al. 2009). In null mice, cerebellar foliation appears delayed with shallower fissures and smaller lobules (Fig. 1G). Perinatal lethality and the largely postnatal development of the cerebellum prevented further investigation of this phenotype with our current mouse model.

A major area of focus for my thesis was the cerebral cortex and its development. By measuring the area of whole mount cerebral cortices, we find that null mice have a significantly decreased cortical area on average compared to the wild type mice (Fig. 1E, $p = 0.009$). We detect no change in cortical thickness in postnatal day 0 (P0) cortical tissue stained with Cresyl Violet,

however cortical layering looks defective with a lack of clearly distinct boundaries between layers (Fig. 1F). Together these findings are consistent with the idea that *Asxl3* is an important Polycomb group gene required for proper development of the brain, among other organs.

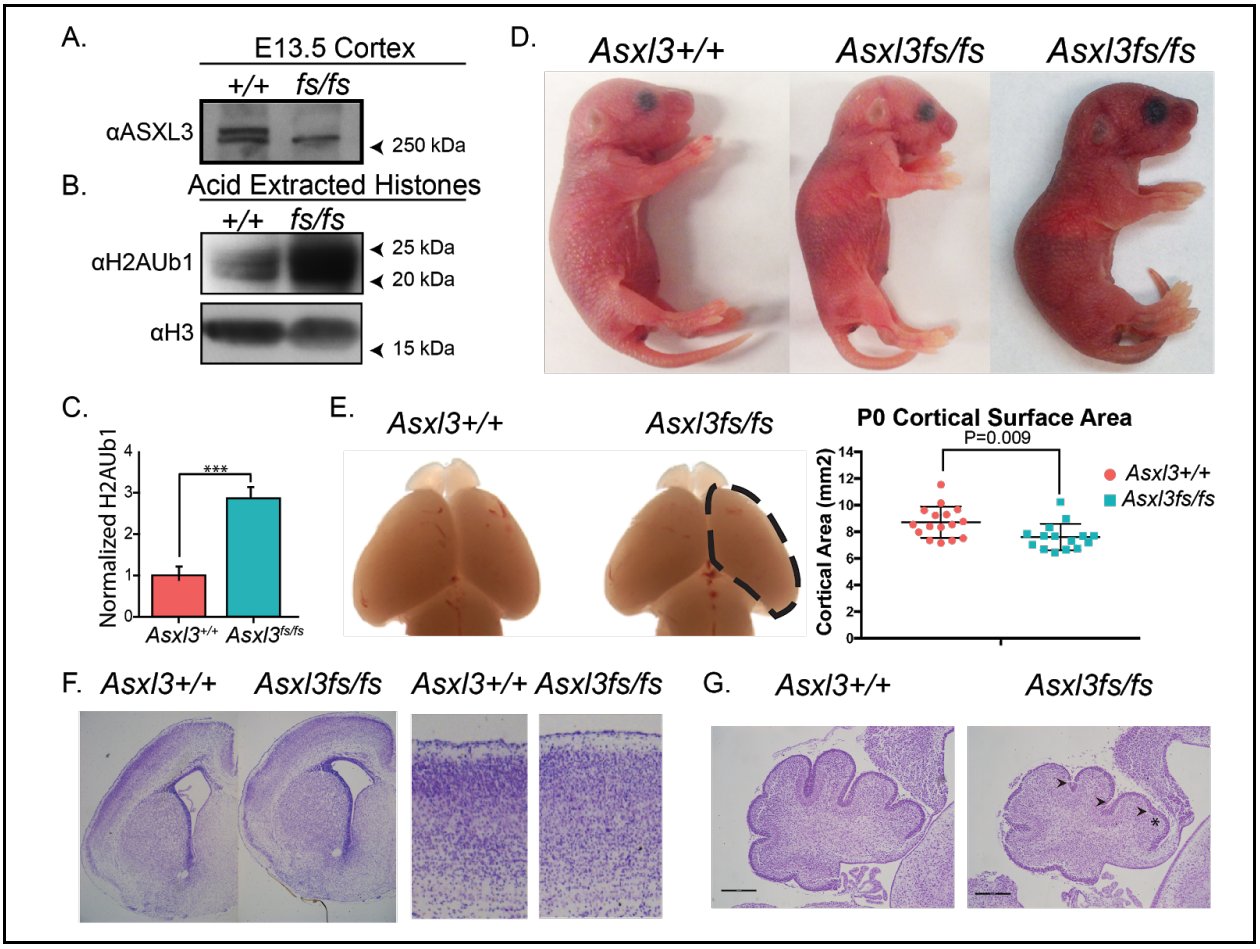

Figure 2: *Asxl3* knockout mouse model and defects in early development
A) Western blot to confirm efficacy of *Asxl3* knockout. B) Western blot for H2AUb1 and H3 on acid extracted histones from E13.5 cortices. C) Quantification of H2AUb1 levels relative to H3 in wild type and null mice. Values are mean ± SEM. D) Appearance of curved back and drooping forelimbs in P0 *Asxl3fs/fs* mice. E) Cortical surface area measurements show decreased cortical area in *Asxl3fs/fs* mice ($p = 0.009$). Values are mean ± SEM. F) Cresyl Violet staining of P0 cerebral cortex G) A reduction in cerebellar foliation is observed in sagittal sections of P2 null mice.

Reduction in Layer 5 Neurons and Defects in Cortical Spinal Tract

During the development of the cerebral cortex, multipotent NPCs differentiate into mature neurons that are organized into 6 layers (L1-6). Neurons within each layer have unique expression profiles that inform their morphology and function required for mature cognitive function and

complex behaviors. Defects in this process can have major downstream consequences on brain function. To investigate potential cortical layering changes in null animals, we perform immunohistochemistry (IHC) for layer specific markers. Using P0 cortical tissue, we probe for TBR1, BCL11B, and SATB2, which mark Layer 6, Layer 5, and Layer 2-4 cells respectively (Fig. 3C). Following quantification of the layer markers, we find no significant difference between the number of TBR1+ layer 6 neurons and SATB2+ layer 2-4 neurons across genotypes (Fig. 3D). We do observe a ~25% reduction in BCL11B+ cells in null cortices (Fig 3D). Interestingly, conditional deletion of Ring1B from the cortex during neurogenesis leads to a ~30% increase in BCL11B+ cells (Morimoto-Suzki et al. 2014). The opposing L5 lamination defects mirror the opposing catalytic activity of PRC1 and PR-DUB, implicating a role for dynamic regulation of H2AUb1 in specifying mature cortical neurons.

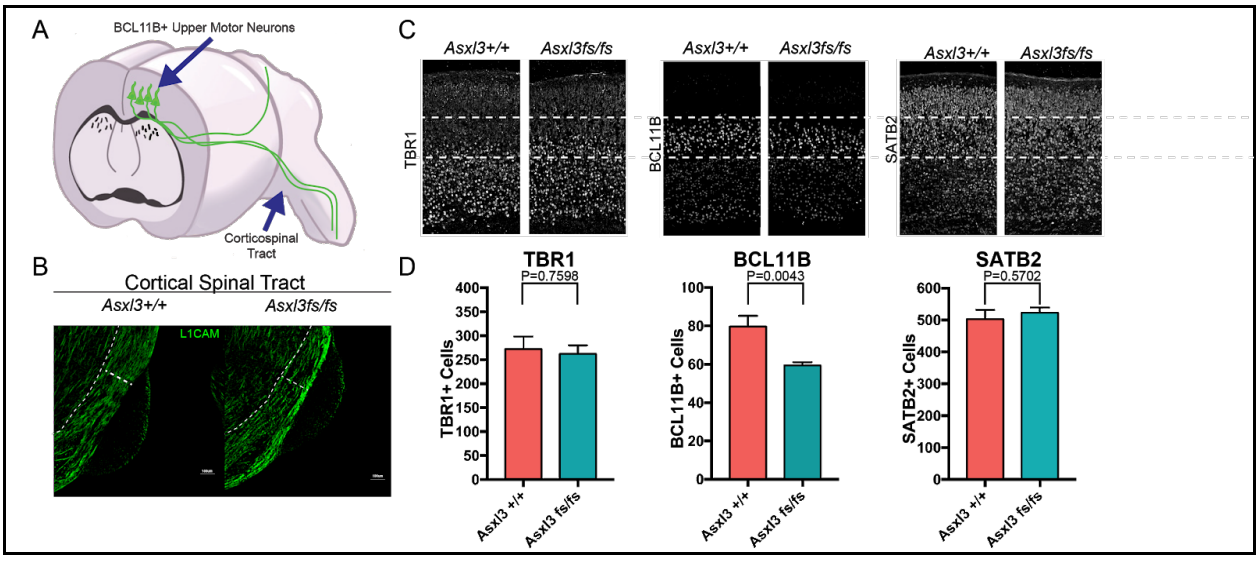

Figure 3: Reduction in layer 5 BCL11B+ neurons and corticospinal tract defects
A) Diagram showing the axons of BCL11B+ L5 neurons projecting subcerebrally via the corticospinal tract B) In *Asxl3fs/fs*, the density of L1CAM stained axons in the corticospinal tract is reduced. C) TBR1 (layer 6), BCL11B (layer 5), and SATB2 (layer 2-4) immunolabeled coronal neocortex sections at P0. D) Quantification of TBR1, BCL11B, and SATB2 positive cells in a radial column. Values are mean ± SEM.

BCL11B+ L5 neurons are upper motor neurons which extend their axons to subcerebral targets in the pons, cerebellum, and spinal cord via the corticospinal tract (Fig. 3A). Based on this

information and our earlier findings, we investigate the corticospinal tract (CST) by staining sagittal sections with L1CAM, a transmembrane protein expressed by neuronal axons. In accordance with reduced BCL11B+ L5 neurons, the density of axons in *Asxl3* null mice is sparse near the pons where the CST typically bundles (Fig. 3B). These results suggest a defect in neurogenesis which leads to disrupted generation of mature neurons and their corresponding axons.

Reduction in Layer 5 Neurons is Caused by a Delay in Differentiation

Since neurons are born from a common pool of progenitors, we hypothesize that a delay in differentiation causes the reduction in L5 neurons. To study this, we use a series of EdU birthdating experiments. Our EdU birthdating protocol involves injecting time pregnant mice with EdU at embryonic stages and collecting pups at P0. EdU is a thymidine analog that incorporates into cells undergoing DNA synthesis. Within the cortex, progenitor cells in the ventricular zone and subventricular zone are the only cells undergoing DNA replication. After the litter is taken and the brains are dissected and stained, the neurons born on the day of the EdU injection can be visualized (Fig. 4A). We use this approach to look at neurons born at two embryonic time points: embryonic day 13 (E13) and embryonic day 14 (E14). These time points are chosen to capture the production of L5 neurons that occurs between E12.5 to E14.5.

Pairing the detection of EdU labeling with immunostaining for BCL11B+ allows us to determine the L5 differentiation dynamics. No appreciable difference between the number of BCL11B+/EdU+ co-labeled cells exists between *Asxl3*+/+ and *Asxl3fs/fs* E13 EdU injected mice (Fig 4B, C, D). In contrast, *Asxl3* null mice receiving EdU treatment at E14 have fewer

BCL11B+/EdU+ co-labeled cells (Fig 4B, C, D). This reduction suggests that a delay in differentiation during neurogenesis underlies the deficit of layer 5 neurons.

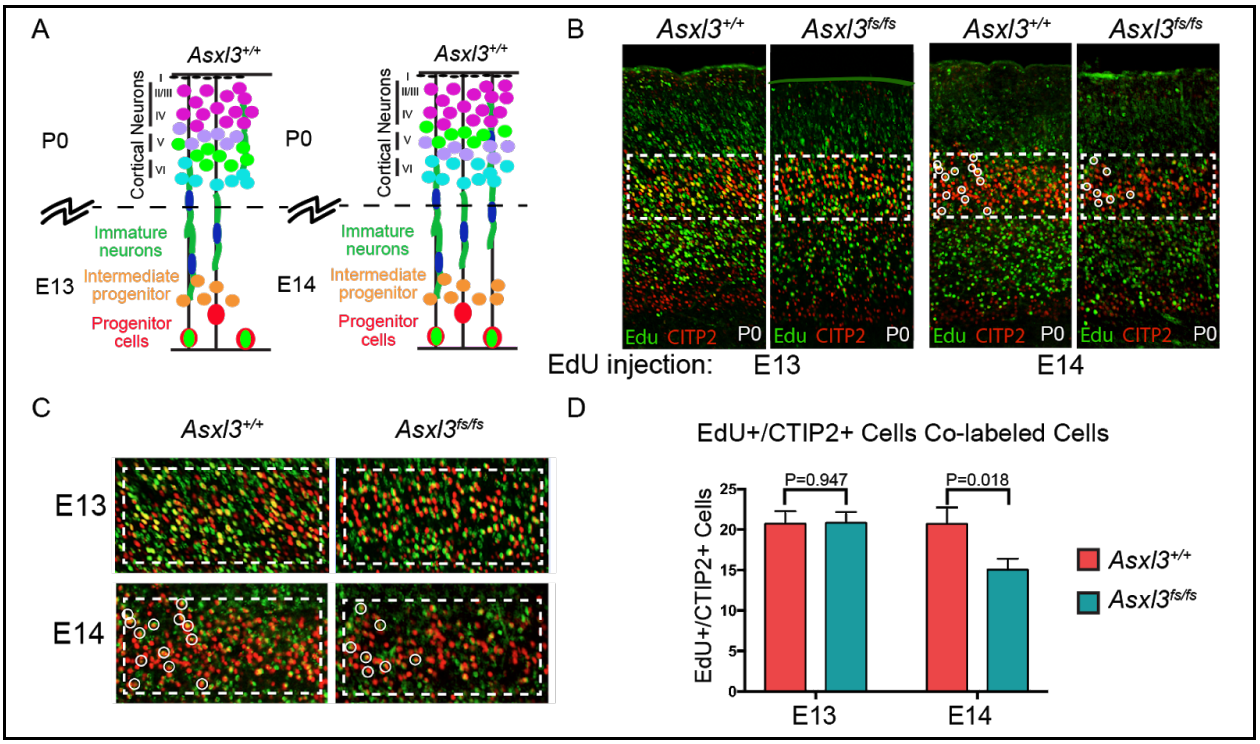

Figure 4: Layer 5 neuron reduction in null mice is the result of a delay in differentiation
A) Schematic depicting EdU birthdating experimental design. Time pregnant mice received EdU treatment at E13 or E14 and visualization of EdU+ cells occurred at P0. B) Representative images of BCL11B+/EdU+ co-labeled cells in P0 cortices of E13 (left) and E14 (right) injected mice. C) Insets of B. White circles mark BCL11B+/EdU+ co-labeled cells. D) No difference exists in the number of co-labeled cells at E13, but there is a reduction at E14 in *Asxl3fs/fs* cortices ($p = 0.018$). Values are mean ± SEM.

Delay in Differentiation Caused by Expansion in NPCs

To delineate the molecular mechanism responsible for impaired differentiation dynamics, we perform single-cell RNA sequencing (scRNA-seq). Using the Seq-Well platform, we conduct scRNA-seq with E13 and E14 wild type and null cortical tissue. Through dimensionality reduction and unsupervised clustering with uniform manifold approximation and projection (UMAP), we identify 12 cell clusters at E13 and 10 cell clusters at E14 (data not shown). Clusters are annotated according to expression of known cell type markers. The identified cell populations correlate to all known major excitatory cell-types present in the E13 and E14 cortex including neural

progenitors, intermediate progenitors, migrating neurons, and excitatory neurons. Comparing the cellular composition of wild type and null samples shows an increase in the proportion of progenitor cells and a decrease in the proportion of intermediate progenitors, immature migrating neurons, and mature deep layer excitatory neurons in null samples at E13 (Fig. 5B). By E14, however, we find that the proportion of progenitor cells is roughly equivalent in both cortices. Instead, the null cortices are showing significantly increased levels of differentiating progenitors when compared to the wild type cortices (Fig. 5B). The expanded progenitor population in null cortices at E13 turns into an expanded differentiating progenitor population in null cortices at E14. By conducting these experiments across multiple developmental time points, we can see that neuronal differentiation is delayed and progenitor multipotency is maintained in *Asxl3* null mice. The dynamics of cell fate restriction appear to be altered in *Asxl3* null mice.

Next, we confirm these composition changes detected by scRNA-seq with IHC in cortical tissue. We perform immunofluorescent staining for SOX2 and TBR2 with E13 cortical tissue. SOX2 marks neural progenitor cells in the ventricular zone and TBR2 marks intermediate progenitors in the sub-ventricular zone (Fig. 5A). Quantification of SOX2+ cells in the medial and lateral neocortices shows increases in the lateral neocortex of null cortices but not in the medial neocortex (Fig. 5D). We also find that the null cortices have decreased TBR2+ cells in the medial neocortex but not in the lateral neocortex. The change in SOX2+ progenitors seems modest compared to the scRNA-seq results. Therefore, we measure the apical length or the perimeter of the ventricles, as shown by the dotted line in (Fig. 5A). Our analysis reveals that null cortices have longer apical lengths relative to their wild type counterparts at E14 (Fig. 5C). Increased apical length indicates lateral expansion of neural progenitor cells and strongly supports the idea that at this time point, null cortices have a larger population of progenitors. The apical lengths of the E15

cortices show no significant difference (data not shown), demonstrating that null cortices have overcome differentiation deficits. Importantly, the trends we observe with our IHC and apical length data correspond with the composition changes detected by scRNA-seq. Evidence from our data shows that null cortices experience an expansion in NPCs with a corresponding delay in neuronal differentiation. These developmental defects in fate specification underlie changes in cortical composition at P0.

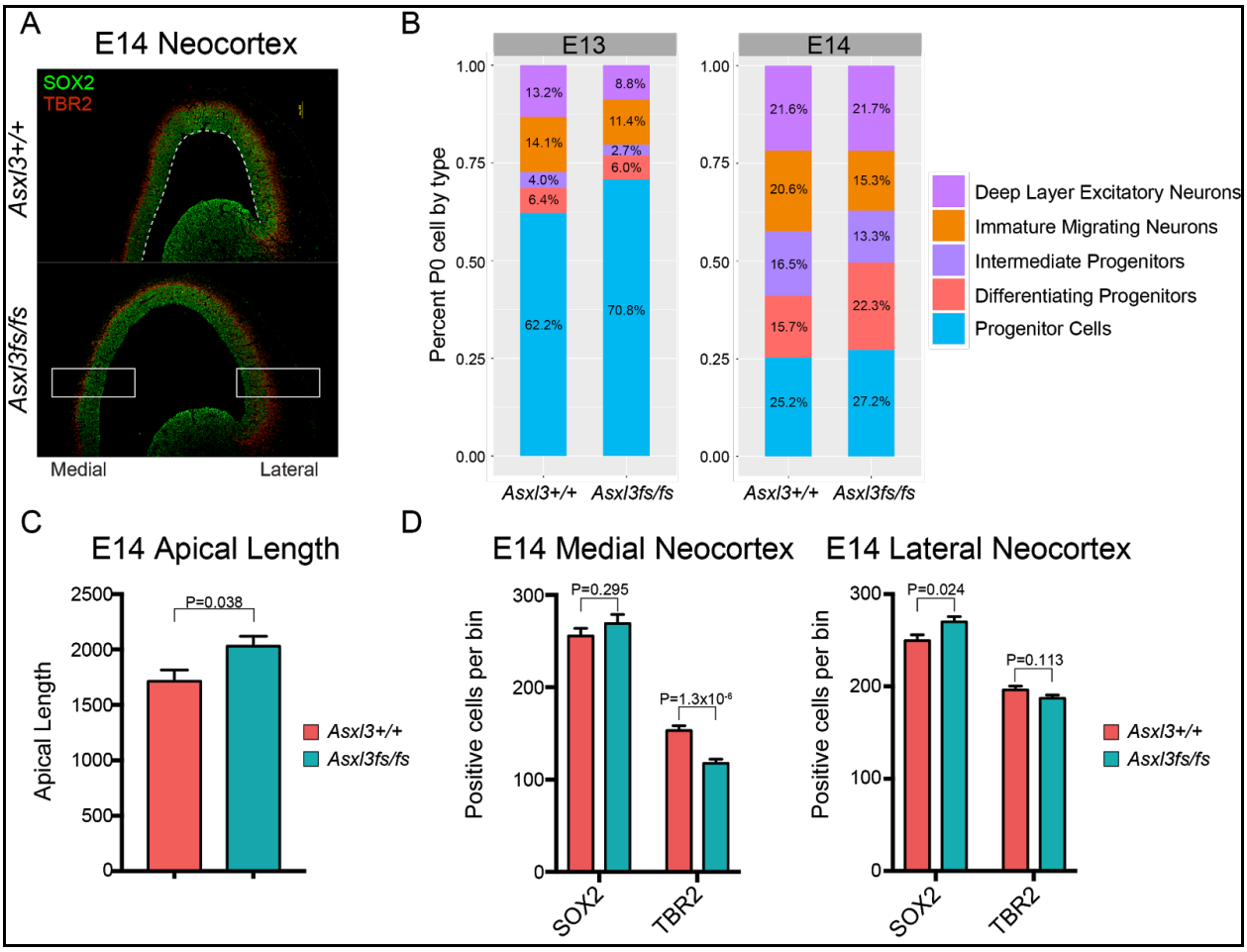

Figure 5: *Asxl3* deficiency inhibits neurogenesis

A) Expression of SOX2 (green) and TBR2 (red) in the E14 neocortex. B) Single-cell RNA sequencing performed with E13 and E14 cortical tissue. Bar graphs depict the cellular composition of major cell types in *Asxl3+/+* and *Asxl3fs/fs* cortices at these time points. C) Apical length (measurement shown in A with dotted line) is increased in E14 *Asxl3fs/fs* mice. Values are mean ± SEM. D) The number of SOX2+ and TBR2+ cells in the E14 medial and lateral neocortex were quantified in bins (white boxes in A). Values are mean ± SEM.

Various Congenital Heart Defects Detected in Null Mice

In addition to the neuronal defects, the *Asxl3fs/fs* and *Asxl3+/fs* mice present with partial penetrance of several congenital heart defects (Fig. 6B). Early imaging and staining, made it clear that the heterozygous and null mice hearts have some degree of cardiac malformation. With whole mount imaging, we observe separated ventricles and a bifid cardiac apex in several P0 hearts (Fig. 6A). These phenotypes are not observed in any of the wild type hearts but are present in a number of the heterozygous and null mice (Fig. 6B). 4.5% of heterozygous mice show separated ventricles, while 16.6% of null mice show separated ventricles and 16.6% have a bifid cardiac apex. Next, we examine heart morphology with hematoxylin and eosin (H&E) staining of serial sections. From our analysis, we find clear septal defects and hypoplastic ventricular cavities in heterozygous and null mice (Fig. 6C). Hypoplastic ventricles is the most penetrant phenotype, with 12.5% of heterozygous mice and 28% of null mice displaying this phenotype (Fig. 6B). In the hearts with hypoplastic ventricular cavities, the ventricles appear incomplete and hypoplastic throughout the entirety of serial sections (data not shown). While this phenotype is observed in both right and left ventricles, right ventricles are more frequently affected. We believe that these congenital heart defects are contributing, at least to some degree, to the perinatal lethality we observed in our mouse litters.

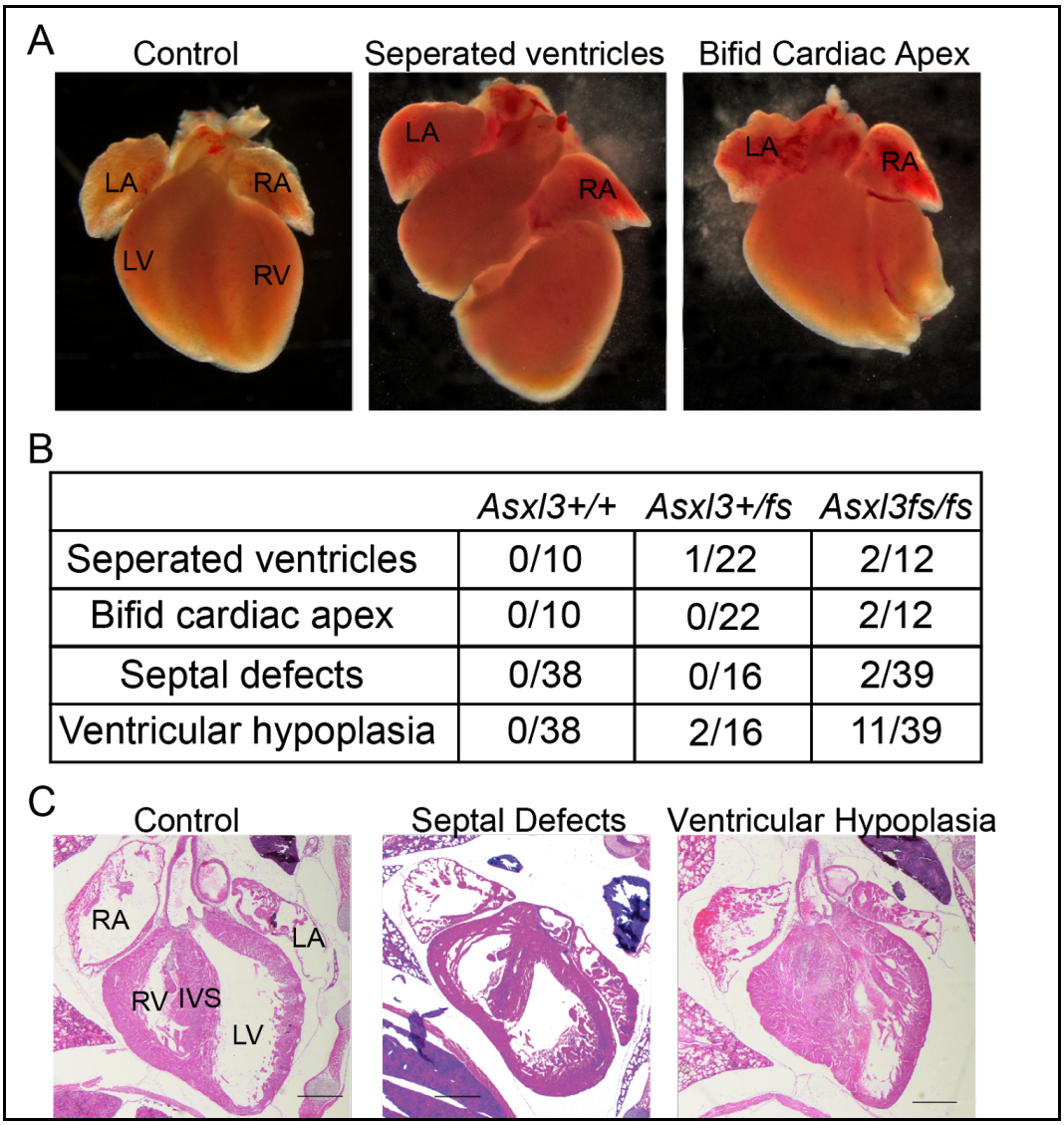

	Asxl3+/+	*Asxl3+/fs*	*Asxl3fs/fs*
Seperated ventricles	0/10	1/22	2/12
Bifid cardiac apex	0/10	0/22	2/12
Septal defects	0/38	0/16	2/39
Ventricular hypoplasia	0/38	2/16	11/39

Figure 6: *Asxl3*-associated congenital heart defects
A) Whole-mount examination of P0 hearts shows separated ventricles and bifid cardiac apex in heterozygous and null mice. B) Penetrance of cardiac abnormalities in *Asxl3+/+*, *Asxl3+/fs*, and *Asxl3fs/fs* P0 mice. C) Representative hematoxylin and eosin staining of transverse P0 sections revealing septal defects and ventricular hypoplasia.

We began to assess the consequences and biological mechanism of the cardiac abnormalities we detect in our *Asxl3* model. Null hearts weigh significantly more than wild type hearts, but no difference is observed in heterozygous mice (Fig. 7A, $p = 0.0083$). Similarly, the heart weight to body weight ratios are increased in null mice relative to the wild type mice, but there is no change in heterozygous mice (Fig. 7B, $p = 0.0070$). Following this analysis, we take a series of morphometric measurements to better understand the structure of the heart following

knockout of *Asxl3*. Specifically, we look at the right wall thickness (RWT), right ventricular lumen width (RVLW), interventricular septum thickness (IVS), left ventricular lumen width (LVLW), and left wall thickness (LWT) (Fig. 7C). The thickness of the two walls and the IVS are statistically equivalent, but the two lumen widths distances are statistically decreased in the null hearts (Fig. 7D, $p < 0.0001$ for RVFW and $p < 0.001$ for LVFW). The reductions in the open lumen space of the ventricles in the null hearts correlate with cardiac defects we saw in the H&E stained cardiac tissue. The phenotype is consistent with the hypoplastic ventricular cavity noted earlier. Morphologically, the outer walls and the septum were not different in the null hearts compared to the wild type hearts.

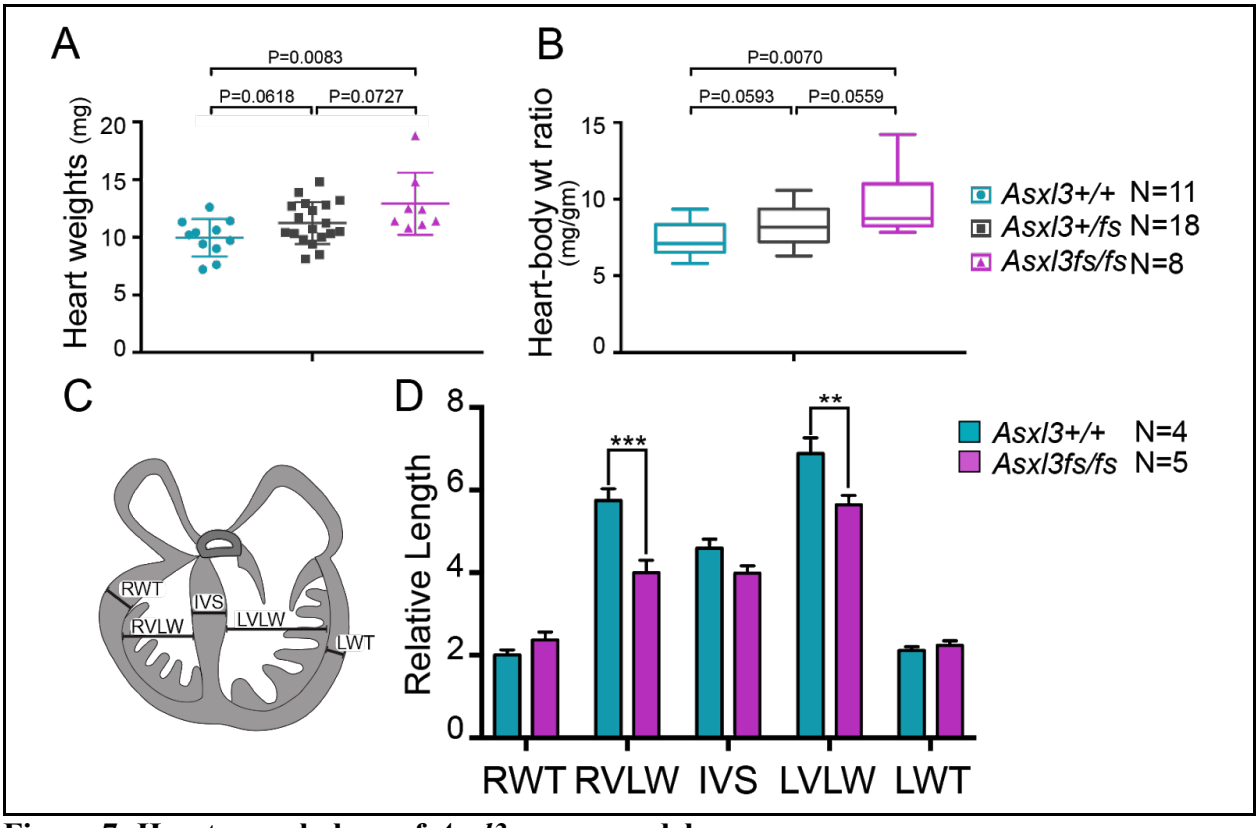

Figure 7: Heart morphology of *Asxl3* mouse model

A) *Asxl3fs/fs* heart weights and B) heart-body weight ratio are significantly increased relative to *Asxl3*+/+ with no significant change in *Asxl3+/fs* mice. C) Schematic diagram of morphometric measurements. D) Graphs depict relative morphometric measurements of P0 hearts. The RVLW and LVLW are significantly reduced in *Asxl3fs/fs* relative to control. RWT, right wall thickness; RVLW, right ventricular lumen width; IVS, interventricular septum; LVLW, left ventricular lumen width; LWT left wall thickness; **$p < 0.001$, ***$p < 0.0001$. Values are mean ± SEM.

Reduced Ventricular Space is Due to Increased Proliferation in Null Hearts

The ventricular walls and septum appear thicker in hearts with hypoplastic ventricular cavities (Fig. 6C). We predict that several mechanisms can be responsible for the changes in chamber development including increased cardiomyocyte size (hypertrophy) or proliferation defects (hyperplasia). Based on the finding that ventricular space is reduced as a result of *Asxl3* knockdown, we hypothesize that cells in the ventricles of null hearts might undergo increased proliferation relative to such cells in wild type hearts. To test this hypothesis, we conduct additional EdU birthdating experiments (Fig. 8A). Time pregnant mice are injected with EdU at E13. A day later, at E14, we analyze the left ventricle, septum, and right ventricle from wild type, heterozygous, and null mice, at which point the heart is actively developing. No significant differences are noted in EdU positive cells in the septum (Fig. 8B). In the left ventricle, the heterozygous and null hearts both show increased levels of EdU positive cells relative to the wild type hearts (Fig. 8B). In the right ventricle, the difference between the heterozygous and wild type hearts is not as significant, but there is a significant increase in the number of EdU positive cells in the null heart relative to the wild type heart (Fig. 8B). Overall, null hearts tend to show increased levels of EdU positive labeled cells in the left and right ventricles at E14. This is consistent with the idea that cell proliferation in these hearts is elevated, leading to the reduction in luminal space noted earlier.

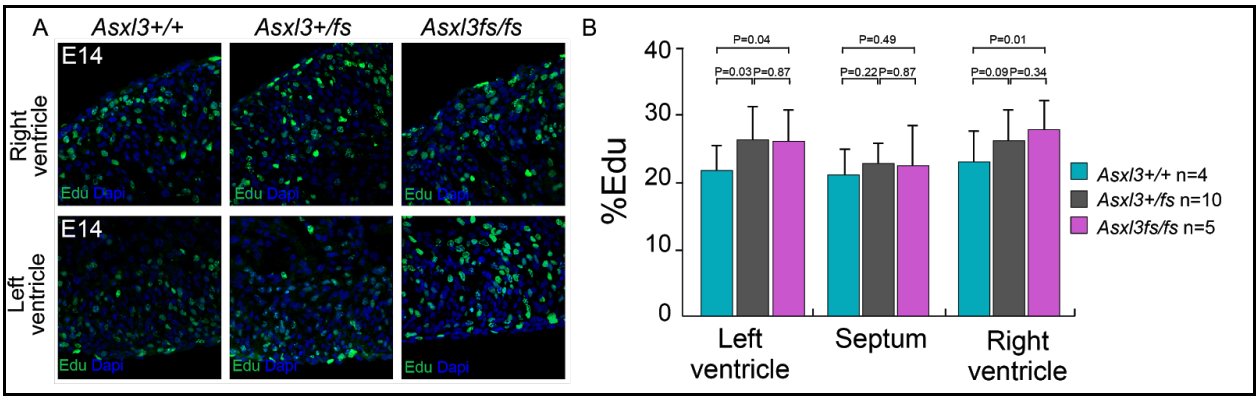

Figure 8: Increased proliferation during heart development
A) EdU labeled E14 left and right ventricles from *Asxl3+/+*, *Asxl3+/fs* and *Asxl3fs/fs* hearts. E13 time pregnant mice were treated with EdU and embryos were collected a day later. B) The percentage of EdU+ cells is increased in E14 *Asxl3+/fs* and *Asxl3fs/fs* left ventricles and *Asxl3fs/fs* right ventricles. Values are mean ± SEM.

Reduction in Vimentin Positive Cells in Null Ventricular Walls

During development, cardiomyocyte proliferation is regulated by interactions with other cells, signaling pathways, transcriptional programs, the extracellular matrix (ECM), and cellular metabolism. Bulk RNA sequencing of E18 hearts reveals dysregulation of extracellular matrix components and corresponding receptors along with cell signaling players in heterozygous and null mice (data not shown). We observe similar results from single-cell RNA sequencing experiments with *ASXL3* edited human embryonic stem cells differentiated toward the cardiac lineage (data not shown). Cardiac fibroblasts deposit the majority of extracellular matrix components in the developing heart. The excreted ECM from embryonic cardiac fibroblasts promotes cardiomyocyte proliferation through ECM receptor signaling pathways (Ieda et al. 2009). Given the ECM changes we detect with RNA-seq and increased proliferation at E14, we choose to investigate potential cardiac fibroblasts deficits. Coronal sections of P0 hearts are immunostained with Vimentin, an intermediate filament protein that marks cardiac fibroblasts (Fig. 9). Vimentin+ cells are quantified in the left and right ventricles as well as the septum (Fig. 9D). Similar to the analysis with the EdU staining, no difference is noted in the number of

Vimentin+ fibroblast in the septum across genotypes. In both ventricles, heterozygous and null samples show significant reductions in the number of Vimentin positive cells relative to wild type samples (Fig. 9A, B, C). These findings support the idea that *Asxl3* functions in cardiac development and suggests that knocking down *Asxl3* may have downstream consequences such as the disrupted collagen and decreased number of cardiac fibroblasts observed in the heterozygous and null hearts.

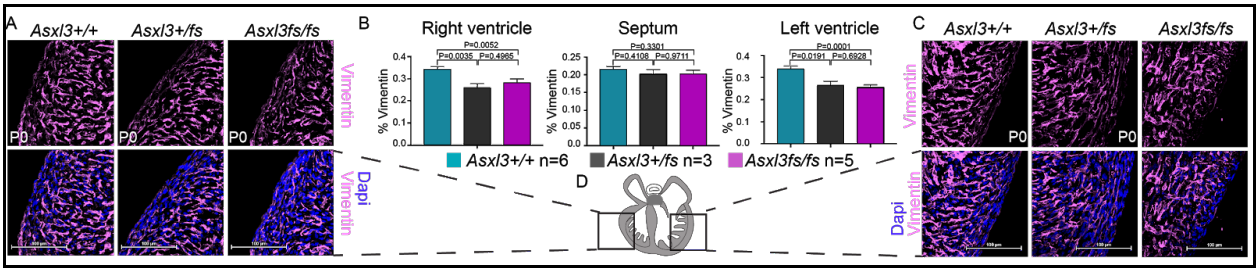

Figure 9: *Asxl3+/fs* and *Asxl3fs/fs* hearts lack VIM+ cells.
A) Immunofluorescent staining of P0 left ventricles with Vimentin and nuclei stained with DAPI. B) Percentage of Vimentin+ cells located in the right ventricle, septum, and left ventricle of *Asxl3+/+*, *Asxl3+/fs* and *Asxl3fs/fs* P0 hearts. Values are mean ± SEM. C) Immunofluorescent staining of P0 right ventricles with Vimentin and nuclei stained with DAPI. D) Schematic of P0 transverse heart sections depicting representative regions of images from A&C.

Our collective data of *Asxl3* in corticogenesis and cardiogenesis, illustrate its fundamental role in regulating developmental processes during organogenesis. In both organ systems, *Asxl3* appears necessary to shape proliferation and differentiation dynamics. Without the function of *Asxl3*, proper fate specification and maintenance of progenitors becomes compromised.

Discussion

During early development, multipotent cells must restrict their fate in a highly regulated manner to ensure the production of the right mature cell types in the right locations. Chromatin plasticity and the dynamic addition and removal of chromatin marks is an important aspect of this fate specification process (Yadav et al. 2018). Certain chromatin marks loosen the structure of the chromatin and nucleosomes, allowing transcription machinery to access the DNA wrapped around the histones. This increases gene transcription in that region. Other chromatin marks result in tightening of the DNA around the histones, blocking transcription machinery from accessing the DNA at that locus. In this way, transcription is repressed. The selective activation and repression of certain genes via chromatin regulation allows for each cell to closely control the differentiation process.

Asxl3 is one of many genes known to be involved with chromatin regulation. ASXL3 helps the PR-DUB complex remove a ubiquitin mark from histone H2A. Previous studies have demonstrated that *de novo* truncating mutations in *Asxl3* are the genetic cause of Bainbridge Ropers Syndrome (BRS), a developmental disorder which presents with symptoms and features consistent with other forms of autism spectrum disorder (ASD) (Bainbridge et al. 2013, Dinwiddie et al. 2013, Srivastava et al. 2016). Early work in my lab has shown that changes in H2A monoubiquitination levels, which are normally regulated by complexes like PRC1 and PR-DUB, were the key molecular pathology of BRS (Srivastava et. al 2016). Compared with other histone marks, there has not been a great deal of research on this particular chromatin mark. Further, much of the current H2AUb1 research uses embryonic stem cells, preventing a molecular understanding during differentiation (Boyer et al. 2006, Endoh et al. 2008, He et al. 2013, Blackledge et al. 2020).

Existing research has not reached a consensus regarding the role of H2AUb1 in regulating gene transcription (Illingworth et al. 2015, Kundu et al. 2018, Blackledge et al. 2020, Tamburri et al. 2020). Some researchers claim that the enzymatic activity of RING1B, a protein which functions in the PRC1 complex to add the ubiquitin mark to H2A, is not necessary for proper embryonic development (Illingworth et al. 2015). However, the *Ring1b* enzymatic null mice exhibited increased embryonic lethality and neurological defects, suggesting that *Ring1b* and proper regulation of H2A monoubiquitination is, in fact, necessary for development. Through the use of an *Asxl3* knockout mouse model, my lab members and I have worked to better characterize the role of ASXL3 and H2AUb1 in early development. We have found that proper regulation of the H2AUb1 is necessary for early embryonic development. Our initial findings showed that *Asxl3* knockout was responsible for elevated levels of H2AUb1 and that this increase in H2AUb1 was also correlated with changes in progenitor behavior and fate specification during the development of multiple organ systems. The work described in this thesis has specifically focused on defects in neuronal development and cardiac development.

Human genetics has revealed many key players in ASD, namely chromatin, transcription and synaptic proteins (De Rubeis et al. 2014, Iossifov et al. 2014, Satterstrom et al. 2020). These proteins are crucial to proper and timely brain development, and loss of function in such proteins is thought to result in neurodevelopmental disorders. ASD may present in vastly different ways, but it is thought that there is a common set of pathways and molecular players whose disruption can be linked to many of these disorders (Parenti et al. 2020). These common pathways are not yet known, and it is unclear how variants in so many genes in different functional groups can lead to similar phenotypes (Sullivan et al. 2019). The genetic heterogeneity has made ASD difficult to study, and research thus far has failed to fully understand what contributes to some of the common

phenotypes. We chose to study *Asxl3* because it is a high confidence syndromic ASD risk gene with high effect size (Satterstrom et al. 2020). Given its role as a chromatin regulator, we predicted that *Asxl3* might act as a hub gene to influence other known ASD risk genes. We hoped studying *Asxl3* would provide insights into how genetics contribute to ASD pathology and the shared pathogenic mechanism that links the functional gene groups. Studying this important gene and understanding its role in causing BRS can provide a solid foundation for further research into other high confidence genes, as well. The work described in this thesis takes a step in that direction.

Previous studies implicate disruptions to the development of deep layer excitatory neurons as the pathogenesis of ASD (Willsey et al. 2013). In accordance with that finding, we determined that loss of ASXL3 results in a reduction in the L5 upper motor neuron population. The reduction in this population was also apparent by the reduced density of the corticospinal tract (CST), which consists of the axons from L5 neurons. CST axons relay important motor signals from the cerebral cortex to targets in the spinal cord. The decrease in CST axons may be responsible for the curved back and drooping forelimb posture of *Asxl3* null mice, a hallmark of neuromuscular defects. Further, we have shown that the reason behind this diminished L5 population is an increased maintenance of neural progenitor cells and a delay in neuronal differentiation. Intriguingly, the dysregulated genes we identified in our scRNA-seq studies were enriched for other known ASD risk genes, with chromatin and transcriptional genes more enriched at early stages and synaptic genes at later developmental stages (data not shown). Together this data suggests that *Asxl3* regulates other ASD risk genes to control NPC behavior during fate specification. Changes in this specification process ultimately have consequences on cortical connections that are responsible for normal neuronal function.

This work establishes the importance of H2AUb1 in the fate specification of NPCs. Experiments with *Ring1b* knockdown showed an opposing phenotype, with L5 neurons being increased (Morimoto-Suzki et al. 2014). The increase in L5 neurons in *Ring1b* null mice and the decrease in L5 neurons in the *Asxl3* null mice were of roughly the same magnitude. Although some studies have suggested that regulation of this chromatin mark is not necessary for development (Illingworth et al. 2015), the opposing lamination defects in *Ring1b* and *Asxl3* null mouse models support a role for H2AUb1 in neural differentiation and development. Currently, we are profiling H2AUb1 across the genomes of E13 NPCs using CUT&RUN analysis, a low input alternative to ChIP-seq. We hope to uncover the epigenomic mechanism of ASXL3-dependent H2AUb1 chromatin remodeling within NPCs necessary for fate determination.

The fate specification process, in which neural progenitor cells (NPCs) sequentially restrict their fate to produce multiple layers of mature neurons, is critical to creating the correct structure and organization of the cerebral cortex (Adam et al. 2020). There is general consensus that the different mature neuron layers arise from a common pool of progenitors. These progenitors go through a highly regulated process in which, at each step, certain fates are restricted but other fates are allowed. The mechanism of selective fate restriction and the control of timing during this process is not fully understood, but our work helps make some headway in this field. Our work provides another data point that suggests that chromatin regulation plays an important role in this process. We showed that loss of ASXL3 alters the behavior of progenitors and leads to changes in the timing of differentiation during early development. Not only is this work applicable to BRS patients and the search for potential therapeutics for BRS patients, but it also provides further insights into the normal corticogenesis process and creates a foundation for studying other neurodevelopmental disorders. ASXL3 is involved with the regulation of various networks, so this

work has implications for many different areas of human genetics research. We are studying some fundamental mechanisms of brain biology. The findings outlined in this thesis contribute to our understanding of ASD biology and also demonstrate a general link between chromatin, transcription, and synaptic genes. When chromatin regulation is disrupted, transcription of certain genes is affected, and this has downstream consequences on many other processes.

Recent studies have shown that mutations in many genes that are known to be associated with neurodevelopmental disorders also contribute risk for congenital heart disease (Jin et al. 2017). Specifically, in CHD patients, damaging *de novo* mutations were enriched in ASD-associated chromatin modifiers, suggesting a link between cardiac and neuronal development (Jin et al. 2017). The findings from our mouse model support this. Loss of function in *Asxl3* resulted in several congenital cardiac abnormalities, the most prominent being hypoplastic ventricles and thickened ventricular walls. This phenotype is reminiscent of the congenital heart disease hypoplastic left heart syndrome (HLHS). Individuals with HLHS have severely thickened left ventricular walls, resulting in reduction of the size of the left ventricular cavity (Grossfeld et al. 2019). The particular phenotype we saw differs slightly in that we see these changes in both the left and right ventricles, as opposed to HLHS which only has these phenotypes in the left ventricular region. There are multiple proposed mechanisms that potentially cause these phenotypes. Some have suggested that reduced blood flow leads to thickening of the ventricular walls and the reduction in the cavities of the heart is attributed to reduced cardiomyocyte proliferation (deAlmeida et al. 2007). More recently it has been suggested that this abnormal structure may be the result of reduced endocardial function and cardiomyocyte hyperplasia (Grossfeld et al. 2019, Miao et al. 2020). We tested these potential mechanisms by investigating proliferation within the developing heart using EdU birthdating experiments. We detected

increased proliferation at E14, consistent with the second model. Cardiac fibroblasts derived from endocardium are known to influence cardiomyocyte proliferation dynamics through extracellular matrix signaling (Ieda et al. 2009). In our studies, we detected decreased numbers of fibroblasts and dysregulated ECM in *Asxl3* null hearts. This lends further support to decreased endocardial function and increased proliferation of cardiomyocytes as the underlying mechanism responsible for the ventricular phenotypes. Importantly, our work is the first to demonstrate a role for chromatin regulation in this disease mechanism.

Past research has also shown that when *Asxl2* is knocked out, thickened ventricular walls and reduced luminal volume is also observed (McGinley et al. 2014). When components of the PRC1 or PRC2 complexes - which work antagonistically to the complexes involving ASXL2 and ASXL3 - are mutated, an opposite phenotype is observed. PRC1 and PRC2 knockout mice display left ventricular non-compaction resulting in thin ventricular walls (Chen et al. 2012, He et al. 2012, Mysliwiec et al. 2011). These studies support the idea that the H2A monoubiquitination regulatory axis is important for cardiac development. When there are insults to the regulation of this chromatin mark, cardiac abnormalities result. It appears that increased H2AUb1 across the genome yields thickened ventricular walls and hypoplastic cavities, whereas decreased H2AUb1 yields thinner ventricular walls and dilated cavities.

Chromatin regulators like ASXL3 have been shown to play important roles in embryonic development. Mutations in other members of the ASXL family, ASXL1 and ASXL2, are linked to developmental disorders and often result in significant abnormalities in organ structure (Hoischen et al. 2011, McGinley et. al 2014, Shashi et al. 2016). Developmental defects in similar organ systems can also be caused by mutations in PRC1 or PRC2 components (He et al. 2012, Beunders et al. 2013, Awad et al. 2013, Pierce et al. 2018, Deevy et al. 2019). Convergence of the

genetic findings provides evidence for the importance of Polycomb regulation in normal development and pathogenesis. Further research into proteins and complexes that modify this chromatin mark can provide significant insight into the processes of organ development and can help elucidate the pathology associated with the various disorders. This kind of work is important not only for expanding our understanding of early development, but also for providing potential targets for therapeutics for the patients with these disorders.

Asxl3 research is relatively new, and there are many further studies that can be conducted. One potential next step would be to determine specifically where ASXL3 binds across the genome. ASXL3 has local effects on the chromatin, not genome-wide effects. Thus, determining where exactly ASXL3 binds can provide insight into the exact DNA regions that are impacted. Those DNA regions and the genes at those loci can be studied further to understand the role of ASXL3 within larger signaling networks. Another potential step would be to do these experiments in human tissues. The experiments described here were performed using mouse models, so the results may not be completely representative of the function of human *ASXL3*. Further research using organoid models may help bridge some of these gaps. This field of research is still in its early stages. Through further research, we can expand our knowledge of how proteins like ASXL3 contribute to early development, allowing us to better understand ASD pathology.

References

Adam, M. A., & Harwell, C. C. (2020). Epigenetic regulation of cortical neurogenesis; orchestrating fate switches at the right time and place. *Current Opinion in Neurobiology*, *63*, 146–153. https://doi.org/10.1016/j.conb.2020.03.012

Ai, S., Yu, X., Li, Y., Peng, Y., Li, C., Yue, Y., Tao, G., Li, C., Pu, W. T., & He, A. (2017). Divergent Requirements for EZH1 in Heart Development Versus Regeneration. *Circulation Research*, *121*(2), 106–112. https://doi.org/10.1161/circresaha.117.311212

Aicher, T. P., Carroll, S., Raddi, G., Gierahn, T., Wadsworth, M. H., Hughes, T. K., Love, C., & Shalek, A. K. (2019). Seq-Well: A Sample-Efficient, Portable Picowell Platform for Massively Parallel Single-Cell RNA Sequencing. *Methods in Molecular Biology*, 111–132. https://doi.org/10.1007/978-1-4939-9240-9_8

Aranda, S., Mas, G., & Di Croce, L. (2015). Regulation of gene transcription by Polycomb proteins. *Science Advances*, *1*(11), e1500737. https://doi.org/10.1126/sciadv.1500737

Arganda-Carreras, I., Kaynig, V., Rueden, C., Eliceiri, K. W., Schindelin, J., Cardona, A., & Sebastian Seung, H. (2017). Trainable Weka Segmentation: a machine learning tool for microscopy pixel classification. *Bioinformatics*, *33*(15), 2424–2426. https://doi.org/10.1093/bioinformatics/btx180

Awad, S., Al-Dosari, M. S., Al-Yacoub, N., Colak, D., Salih, M. A., Alkuraya, F. S., & Poizat, C. (2013). Mutation in PHC1 implicates chromatin remodeling in primary microcephaly pathogenesis. *Human Molecular Genetics*, *22*(11), 2200–2213. https://doi.org/10.1093/hmg/ddt072

Bailey, A. (1998). A clinicopathological study of autism. *Brain*, *121*(5), 889–905. https://doi.org/10.1093/brain/121.5.889

Bailey, A., Le Couteur, A., Gottesman, I., Bolton, P., Simonoff, E., Yuzda, E., & Rutter, M. (1995). Autism as a strongly genetic disorder: evidence from a British twin study. *Psychological Medicine*, *25*(1), 63–77. https://doi.org/10.1017/s0033291700028099

Bainbridge, M. N., Hu, H., Muzny, D. M., Musante, L., Lupski, J. R., Graham, B. H., Chen, W., Gripp, K. W., Jenny, K., Wienker, T. F., Yang, Y., Sutton, V. R., Gibbs, R. A., & Ropers, H. H. (2013). De novo truncating mutations in ASXL3 are associated with a novel clinical phenotype with similarities to Bohring-Opitz syndrome. *Genome Medicine*, *5*(2), 11. https://doi.org/10.1186/gm415

Balasubramanian, M., Schirwani, S., Adam, M., Ardinger, H., Pagon, R., Wallace, S., Bean, L., Stephens, K., & Amemiya, A. (2020). ASXL3-Related Disorder. In *GeneReviews*. University of Washington, Seattle.

Beunders, G., Voorhoeve, E., Golzio, C., Pardo, L. M., Rosenfeld, J. A., Talkowski, M. E., Simonic, I., Lionel, A. C., Vergult, S., Pyatt, R. E., van de Kamp, J., Nieuwint, A., Weiss, M. M., Rizzu, P., Verwer, L. E. N. I., van Spaendonk, R. M. L., Shen, Y., Wu, B.-, Yu, T., … Sistermans, E. A. (2013). Exonic Deletions in AUTS2 Cause a Syndromic Form of Intellectual Disability and Suggest a Critical Role for the C Terminus. *The American Journal of Human Genetics*, *92*(2), 210–220. https://doi.org/10.1016/j.ajhg.2012.12.011

Blackledge, N. P., Fursova, N. A., Kelley, J. R., Huseyin, M. K., Feldmann, A., & Klose, R. J. (2020). PRC1 Catalytic Activity Is Central to Polycomb System Function. *Molecular Cell*, *77*(4), 857-874.e9. https://doi.org/10.1016/j.molcel.2019.12.001

Boyer, L. A., Plath, K., Zeitlinger, J., Brambrink, T., Medeiros, L. A., Lee, T. I., Levine, S. S., Wernig, M., Tajonar, A., Ray, M. K., Bell, G. W., Otte, A. P., Vidal, M., Gifford, D. K., Young, R. A., & Jaenisch, R. (2006). Polycomb complexes repress developmental regulators in murine embryonic stem cells. *Nature*, *441*(7091), 349–353. https://doi.org/10.1038/nature04733

Bruneau, B. G. (2013). Signaling and Transcriptional Networks in Heart Development and Regeneration. *Cold Spring Harbor Perspectives in Biology*, *5*(3), a008292. https://doi.org/10.1101/cshperspect.a008292

Buckingham, M., Meilhac, S., & Zaffran, S. (2005). Building the mammalian heart from two sources of myocardial cells. *Nature Reviews Genetics*, *6*(11), 826–835. https://doi.org/10.1038/nrg1710

Chen, L., Ma, Y., Kim, E. Y., Yu, W., Schwartz, R. J., Qian, L., & Wang, J. (2012). Conditional Ablation of Ezh2 in Murine Hearts Reveals Its Essential Roles in Endocardial Cushion Formation, Cardiomyocyte Proliferation and Survival. *PLoS ONE*, *7*(2), e31005. https://doi.org/10.1371/journal.pone.0031005

Chittock, E. C., Latwiel, S., Miller, T. C. R., & Müller, C. W. (2017). Molecular architecture of polycomb repressive complexes. *Biochemical Society Transactions*, *45*(1), 193–205. https://doi.org/10.1042/bst20160173

Chrispijn, N. D., Elurbe, D. M., Mickoleit, M., Aben, M., de Bakker, D. E. M., Andralojc, K. M., Huisken, J., Bakkers, J., & Kamminga, L. M. (2019). Loss of the Polycomb group protein Rnf2 results in derepression of tbx-transcription factors and defects in embryonic and cardiac development. *Scientific Reports*, *9*(1). https://doi.org/10.1038/s41598-019-40867-1

Corley, M., & Kroll, K. L. (2014). The roles and regulation of Polycomb complexes in neural development. *Cell and Tissue Research*, *359*(1), 65–85. https://doi.org/10.1007/s00441-014-2011-9

Cui, Y., Zheng, Y., Liu, X., Yan, L., Fan, X., Yong, J., Hu, Y., Dong, J., Li, Q., Wu, X., Gao, S., Li, J., Wen, L., Qiao, J., & Tang, F. (2019). Single-Cell Transcriptome Analysis Maps the Developmental Track of the Human Heart. *Cell Reports*, *26*(7), 1934-1950.e5. https://doi.org/10.1016/j.celrep.2019.01.079

De Rubeis, S., He, X., Goldberg, A. *et al.* Synaptic, transcriptional and chromatin genes disrupted in autism. *Nature*, *515*, 209–215 (2014). https://doi.org/10.1038/nature13772

deAlmeida, A., McQuinn, T., & Sedmera, D. (2007). Increased Ventricular Preload Is Compensated by Myocyte Proliferation in Normal and Hypoplastic Fetal Chick Left Ventricle. *Circulation Research*, *100*(9), 1363–1370. https://doi.org/10.1161/01.res.0000266606.88463.cb

Deevy, O., & Bracken, A. P. (2019). PRC2 functions in development and congenital disorders. *Development*, *146*(19), dev181354. https://doi.org/10.1242/dev.181354

DeLaughter, D. M., Bick, A. G., Wakimoto, H., McKean, D., Gorham, J. M., Kathiriya, I. S., Hinson, J. T., Homsy, J., Gray, J., Pu, W., Bruneau, B. G., Seidman, J. G., & Seidman, C. E. (2016). Single-Cell Resolution of Temporal Gene Expression during Heart Development. *Developmental Cell*, *39*(4), 480–490. https://doi.org/10.1016/j.devcel.2016.10.001

Delgado-Olguín, P., Huang, Y., Li, X., Christodoulou, D., Seidman, C. E., Seidman, J. G., Tarakhovsky, A., & Bruneau, B. G. (2012). Epigenetic repression of cardiac progenitor

gene expression by Ezh2 is required for postnatal cardiac homeostasis. *Nature Genetics*, *44*(3), 343–347. https://doi.org/10.1038/ng.1068

Desai, A.R. and S.K. McConnell, Progressive restriction in fate potential by neural progenitors during cerebral cortical development.Development, 2000. 127(13): p. 2863-72

Dinwiddie, D. L., Soden, S. E., Saunders, C. J., Miller, N. A., Farrow, E. G., Smith, L. D., & Kingsmore, S. F. (2013). De novo frameshift mutation in ASXL3 in a patient with global developmental delay, microcephaly, and craniofacial anomalies. *BMC Medical Genomics*, *6*(1), 1. https://doi.org/10.1186/1755-8794-6-32

Endoh, M., Endo, T. A., Endoh, T., Fujimura, Y.-, Ohara, O., Toyoda, T., Otte, A. P., Okano, M., Brockdorff, N., Vidal, M., & Koseki, H. (2008). Polycomb group proteins Ring1A/B are functionally linked to the core transcriptional regulatory circuitry to maintain ES cell identity. *Development*, *135*(8), 1513–1524. https://doi.org/10.1242/dev.014340

Fu, F., Li, R., Lei, T.-, Wang, D., Yang, X., Han, J., Pan, M., Zhen, L., Li, J., Li, F.-, Jing, X.-, Li, D.-, & Liao, C. (2020). Compound heterozygous mutation of the ASXL3 gene causes autosomal recessive congenital heart disease. *Human Genetics*, 1. https://doi.org/10.1007/s00439-020-02200-z

Geschwind, D. H., & Levitt, P. (2007). Autism spectrum disorders: developmental disconnection syndromes. *Current Opinion in Neurobiology*, *17*(1), 103–111. https://doi.org/10.1016/j.conb.2007.01.009

Gierahn, T., Wadsworth, M., Hughes, T. *et al.* Seq-Well: portable, low-cost RNA sequencing of single cells at high throughput. *Nat Methods, 14*(4), 395–398 (2017). https://doi.org/10.1038/nmeth.4179

Grossfeld, P., Nie, S., Lin, L., Wang, L., & Anderson, R. (2019). Hypoplastic Left Heart Syndrome: A New Paradigm for an Old Disease? *Journal of Cardiovascular Development and Disease*, *6*(1), 10. https://doi.org/10.3390/jcdd6010010

He, A., Ma, Q., Cao, J., von Gise, A., Zhou, P., Xie, H., Zhang, B., Hsing, M., Christodoulou, D. C., Cahan, P., Daley, G. Q., Kong, S. W., Orkin, S. H., Seidman, C. E., Seidman, J. G., & Pu, W. T. (2012). Polycomb Repressive Complex 2 Regulates Normal Development of the Mouse Heart. *Circulation Research*, *110*(3), 406–415. https://doi.org/10.1161/circresaha.111.252205

He, A., & Pu, W. T. (2012). Mature Cardiomyocytes Recall Their Progenitor Experience Via Polycomb Repressive Complex 2. *Circulation Research*, *111*(2), 162–164. https://doi.org/10.1161/res.0b013e3182635cbf

He, J., Shen, L., Wan, M., Taranova, O., Wu, H., & Zhang, Y. (2013). Kdm2b maintains murine embryonic stem cell status by recruiting PRC1 complex to CpG islands of developmental genes. *Nature Cell Biology*, *15*(4), 373–384. https://doi.org/10.1038/ncb2702

Hoischen, A., van Bon, B., Rodríguez-Santiago, B. *et al. De novo* nonsense mutations in *ASXL1* cause Bohring-Opitz syndrome. *Nat Genet, 43*, 729–731 (2011). https://doi.org/10.1038/ng.868

Homsy, J., Zaidi, S., Shen, Y., Ware, J. S., Samocha, K. E., Karczewski, K. J., DePalma, S. R., McKean, D., Wakimoto, H., Gorham, J., Jin, S. C., Deanfield, J., Giardini, A., Porter, G. A., Kim, R., Bilguvar, K., Lopez-Giraldez, F., Tikhonova, I., Mane, S., … Chung, W. K. (2015). De novo mutations in congenital heart disease with neurodevelopmental and other congenital anomalies. *Science*, *350*(6265), 1262–1266. https://doi.org/10.1126/science.aac9396

Hultman, C. M., & Sparén, P. (2004). Autism—prenatal insults or an epiphenomenon of a strongly genetic disorder? *The Lancet*, *364*(9433), 485–487. https://doi.org/10.1016/s0140-6736(04)16825-6

Ieda, M., Tsuchihashi, T., Ivey, K. N., Ross, R. S., Hong, T.-T., Shaw, R. M., & Srivastava, D. (2009). Cardiac Fibroblasts Regulate Myocardial Proliferation through β1 Integrin Signaling. *Developmental Cell*, *16*(2), 233–244. https://doi.org/10.1016/j.devcel.2008.12.007

Illingworth, R. S., Moffat, M., Mann, A. R., Read, D., Hunter, C. J., Pradeepa, M. M., Adams, I. R., & Bickmore, W. A. (2015). The E3 ubiquitin ligase activity of RING1B is not essential for early mouse development. *Genes & Development*, *29*(18), 1897–1902. https://doi.org/10.1101/gad.268151.115

Iossifov, I., O'Roak, B., Sanders, S. *et al.* The contribution of *de novo* coding mutations to autism spectrum disorder. *Nature*, *515*, 216–221 (2014). https://doi.org/10.1038/nature13908

Jin, S. C., Homsy, J., Zaidi, S., Lu, Q., Morton, S., DePalma, S. R., Zeng, X., Qi, H., Chang, W., Sierant, M. C., Hung, W.-C., Haider, S., Zhang, J., Knight, J., Bjornson, R. D., Castaldi, C., Tikhonoa, I. R., Bilguvar, K., Mane, S. M., … Brueckner, M. (2017). Contribution of rare inherited and de novo variants in 2,871 congenital heart disease probands. *Nature Genetics*, *49*(11), 1593–1601. https://doi.org/10.1038/ng.3970

Katoh, M., & Katoh, M. (2004). Identification and characterization of ASXL3 gene in silico. *International Journal of Oncology*, *24*(6), 1617–1622. https://doi.org/10.3892/ijo.24.6.1617

Kemper, T. L., & Bauman, M. (1998). Neuropathology of Infantile Autism. *Journal of Neuropathology and Experimental Neurology*, *57*(7), 645–652. https://doi.org/10.1097/00005072-199807000-00001

Kundu, S., Ji, F., Sunwoo, H., Jain, G., Lee, J. T., Sadreyev, R. I., Dekker, J., & Kingston, R. E. (2018). Polycomb Repressive Complex 1 Generates Discrete Compacted Domains that Change during Differentiation. *Molecular Cell*, *71*(1), 191. https://doi.org/10.1016/j.molcel.2018.06.022

Lee, S., Lee, J. W., & Lee, S.-K. (2012). UTX, a Histone H3-Lysine 27 Demethylase, Acts as a Critical Switch to Activate the Cardiac Developmental Program. *Developmental Cell*, *22*(1), 25–37. https://doi.org/10.1016/j.devcel.2011.11.009

Macosko, E. Z., Basu, A., Satija, R., Nemesh, J., Shekhar, K., Goldman, M., Tirosh, I., Bialas, A. R., Kamitaki, N., Martersteck, E. M., Trombetta, J. J., Weitz, D. A., Sanes, J. R., Shalek, A. K., Regev, A., & McCarroll, S. A. (2015). Highly Parallel Genome-wide Expression Profiling of Individual Cells Using Nanoliter Droplets. *Cell*, *161*(5), 1202–1214. https://doi.org/10.1016/j.cell.2015.05.002

McConnell, S. K. (1995). Constructing the cerebral cortex: Neurogenesis and fate determination. *Neuron*, *15*(4), 761–768. https://doi.org/10.1016/0896-6273(95)90168-x

McGinley, A. L., Li, Y., Deliu, Z., & Wang, Q. T. (2014). Additional sex combs-likefamily genes are required for normal cardiovascular development. *Genesis*, *52*(7), 671–686. https://doi.org/10.1002/dvg.22793

Miao, Y., Tian, L., Martin, M., Paige, S. L., Galdos, F. X., Li, J., Klein, A., Zhang, H., Ma, N., Wei, Y., Stewart, M., Lee, S., Moonen, J.-R., Zhang, B., Grossfeld, P., Mital, S., Chitayat, D., Wu, J. C., Rabinovitch, M., … Gu, M. (2020). Intrinsic Endocardial Defects

Contribute to Hypoplastic Left Heart Syndrome. *Cell Stem Cell*, *27*(4), 574-589.e8. https://doi.org/10.1016/j.stem.2020.07.015

Miquerol, L., & Kelly, R. G. (2012). Organogenesis of the vertebrate heart. *Wiley Interdisciplinary Reviews: Developmental Biology*, *2*(1), 17–29. https://doi.org/10.1002/wdev.68

Morimoto-Suzki, N., Hirabayashi, Y., Tyssowski, K., Shinga, J., Vidal, M., Koseki, H., & Gotoh, Y. (2014). The polycomb component Ring1B regulates the timed termination of subcerebral projection neuron production during mouse neocortical development. *Development*, *141*(22), 4343–4353. https://doi.org/10.1242/dev.112276

Mysliwiec, M. R., Bresnick, E. H., & Lee, Y. (2011). Endothelial Jarid2/Jumonji Is Required for Normal Cardiac Development and Proper Notch1 Expression. *Journal of Biological Chemistry*, *286*(19), 17193–17204. https://doi.org/10.1074/jbc.m110.205146

Olson, E. N. (2006). Gene Regulatory Networks in the Evolution and Development of the Heart. *Science*, *313*(5795), 1922–1927. https://doi.org/10.1126/science.1132292

Parenti, I., Rabaneda, L.G., Schoen, H., & Novarino, G. (2020). Neurodevelopmental Disorders: From Genetics to Functional Pathways. *Trends in Neurosciences*, *43*(8), 608-621. https://doi.org/10.1016/j.tins.2020.05.004

Pierce, S. B., Stewart, M. D., Gulsuner, S., Walsh, T., Dhall, A., McClellan, J. M., Klevit, R. E., & King, M.-C. (2018). De novo mutation in RING1 with epigenetic effects on neurodevelopment. *Proceedings of the National Academy of Sciences*, *115*(7), 1558–1563. https://doi.org/10.1073/pnas.1721290115

Satterstrom, F. K., Kosmicki, J. A., Wang, J., Breen, M. S., De Rubeis, S., An, J.-Y., Peng, M., Collins, R., Grove, J., Klei, L., Stevens, C., Reichert, J., Mulhern, M. S., Artomov, M.,

Gerges, S., Sheppard, B., Xu, X., Bhaduri, A., Norman, U., … Walters, R. K. (2020). Large-Scale Exome Sequencing Study Implicates Both Developmental and Functional Changes in the Neurobiology of Autism. *Cell*, *180*(3), 568-584.e23. https://doi.org/10.1016/j.cell.2019.12.036

Scheuermann, J. C., de Ayala Alonso, A. G., Oktaba, K., Ly-Hartig, N., McGinty, R. K., Fraterman, S., Wilm, M., Muir, T. W., & Müller, J. (2010). Histone H2A deubiquitinase activity of the Polycomb repressive complex PR-DUB. *Nature*, *465*(7295), 243–247. https://doi.org/10.1038/nature08966

Schuettengruber, B., Bourbon, H.-M., Di Croce, L., & Cavalli, G. (2017). Genome Regulation by Polycomb and Trithorax: 70 Years and Counting. *Cell*, *171*(1), 34–57. https://doi.org/10.1016/j.cell.2017.08.002

Shashi, V., Pena, L. D. M., Kim, K., Burton, B., Hempel, M., Schoch, K., Walkiewicz, M., McLaughlin, H. M., Cho, M., Stong, N., Hickey, S. E., Shuss, C. M., Freemark, M. S., Bellet, J. S., Keels, M. A., Bonner, M. J., El-Dairi, M., Butler, M., Kranz, P. G., … Cogan, J. D. (2016). De Novo Truncating Variants in ASXL2 Are Associated with a Unique and Recognizable Clinical Phenotype. *The American Journal of Human Genetics*, *99*(4), 991–999. https://doi.org/10.1016/j.ajhg.2016.08.017

Shen, Q., Wang, Y., Dimos, J. T., Fasano, C. A., Phoenix, T. N., Lemischka, I. R., Ivanova, N. B., Stifani, S., Morrisey, E. E., & Temple, S. (2006). The timing of cortical neurogenesis is encoded within lineages of individual progenitor cells. *Nature Neuroscience*, *9*(6), 743–751. https://doi.org/10.1038/nn1694

Shirai, M., Osugi, T., Koga, H., Kaji, Y., Takimoto, E., Komuro, I., Hara, J., Miwa, T., Yamauchi-Takihara, K., & Takihara, Y. (2002). The Polycomb-group gene Rae28

sustains Nkx2.5/Csx expression and is essential for cardiac morphogenesis. *Journal of Clinical Investigation*, *110*(2), 177–184. https://doi.org/10.1172/jci0214839

Shirley, Dame Stephanie. "Challenges to Autism Research." *Journal of the Royal Society of Medicine*, vol. 98, no. 11, 2005, pp. 523–525

Srivastava, Anshika, et al. "De novo dominant ASXL3 mutations Alter H2A Deubiquitination and Transcription in Bainbridge–Ropers Syndrome." *Human Molecular Genetics*, vol. 25, no. 3, 2016, pp. 597–608., doi:10.1093/hmg/ddv499.

Srivastava, A., McGrath, B., & Bielas, S. L. (2017). Histone H2A Monoubiquitination in Neurodevelopmental Disorders. *Trends in Genetics*, *33*(8), 566–578. https://doi.org/10.1016/j.tig.2017.06.002

Srivastava, D. (2006). Making or Breaking the Heart: From Lineage Determination to Morphogenesis. *Cell*, *126*(6), 1037–1048. https://doi.org/10.1016/j.cell.2006.09.003

Sullivan, J. M., De Rubeis, S., & Schaefer, A. (2019). Convergence of spectrums: neuronal gene network states in autism spectrum disorder. *Current Opinion in Neurobiology*, *59*, 102–111. https://doi.org/10.1016/j.conb.2019.04.011

Tamburri, S., Lavarone, E., Fernández-Pérez, D., Conway, E., Zanotti, M., Manganaro, D., & Pasini, D. (2020). Histone H2AK119 Mono-Ubiquitination Is Essential for Polycomb-Mediated Transcriptional Repression. *Molecular Cell*, *77*(4), 840-856.e5. https://doi.org/10.1016/j.molcel.2019.11.021

Triedman JK, Newburger JW. Trends in congenital heart disease: the next decade. Circulation. 2016;133:2716–2733. doi: 10.1161/CIRCULATIONAHA.116.023544.

Voineagu, I., Wang, X., Johnston, P., Lowe, J. K., Tian, Y., Horvath, S., Mill, J., Cantor, R. M., Blencowe, B. J., & Geschwind, D. H. (2011). Transcriptomic analysis of autistic brain

reveals convergent molecular pathology. *Nature*, *474*(7351), 380–384. https://doi.org/10.1038/nature10110

Willsey, A. J., Sanders, S. J., Li, M., Dong, S., Tebbenkamp, A. T., Muhle, R. A., Reilly, S. K., Lin, L., Fertuzinhos, S., Miller, J. A., Murtha, M. T., Bichsel, C., Niu, W., Cotney, J., Ercan-Sencicek, A. G., Gockley, J., Gupta, A. R., Han, W., He, X., & State, M. W. (2013). Coexpression Networks Implicate Human Midfetal Deep Cortical Projection Neurons in the Pathogenesis of Autism. *Cell*, *155*(5), 997–1007. https://doi.org/10.1016/j.cell.2013.10.020

Yadav, T., Quivy, J.-P., & Almouzni, G. (2018). Chromatin plasticity: A versatile landscape that underlies cell fate and identity. *Science*, *361*(6409), 1332–1336. https://doi.org/10.1126/science.aat8950

Zaidi, S., Choi, M., Wakimoto, H., Ma, L., Jiang, J., Overton, J. D., Romano-Adesman, A., Bjornson, R. D., Breitbart, R. E., Brown, K. K., Carriero, N. J., Cheung, Y. H., Deanfield, J., DePalma, S., Fakhro, K. A., Glessner, J., Hakonarson, H., Italia, M. J., Kaltman, J. R., & Lifton, R. P. (2013). De novo mutations in histone-modifying genes in congenital heart disease. *Nature*, *498*(7453), 220–223. https://doi.org/10.1038/nature12141